

FPC-VLA: A Vision-Language-Action Framework with a Supervisor for Failure Prediction and Correction

Yifan Yang^{1,2}, Zhixiang Duan^{2†}, Tianshi Xie², Fuyu Cao^{3,2}, Pinxi Shen², Peili Song¹, Piaopiao Jin², Guokang Sun², Shaoqing Xu^{2,4}, Yangwei You², and Jingtai Liu^{1*}, Senior Member, IEEE.

Abstract—Robotic manipulation is a fundamental component of automation. However, traditional perception-planning pipelines often fall short in open-ended tasks due to limited flexibility, while the architecture of a single end-to-end Vision-Language-Action (VLA) offers promising capabilities but lacks crucial mechanisms for anticipating and recovering from failure. To address these challenges, we propose FPC-VLA, a dual-model framework that integrates VLA with a supervisor for failure prediction and correction. The supervisor evaluates action viability through vision-language queries and generates corrective strategies when risks arise, trained efficiently without manual labeling. A similarity-guided fusion module further refines actions by leveraging past predictions. Evaluation results on multiple simulation platforms (SIMPLER and LIBERO) and robot embodiments (WidowX, Google Robot, Franka) show that FPC-VLA outperforms state-of-the-art models in both zero-shot and fine-tuned settings. By activating the supervisor only at keyframes, our approach significantly increases task success rates with minimal impact on execution time. Successful real-world deployments on diverse, long-horizon tasks confirm FPC-VLA’s strong generalization and practical utility for building more reliable autonomous systems. Our project page is <https://fpcvla.github.io/>.

I. INTRODUCTION

Robot manipulation is crucial for advancing automation in industries like manufacturing, logistics and healthcare [1], [2]. Traditional approaches follow a two-stage “perception-planning” pipeline: estimating object poses and predefined grasp points [3], [4], then generating motion trajectories. This requires explicit recognition and geometric modeling, assuming prior knowledge of target objects, which limits flexibility in open-ended tasks. Additionally, pose estimation and grasp-point labeling often fail under occlusion, clutter, or with novel objects, causing errors in perception that propagate to planning and lead to unreliable actions.

Unlike traditional modular pipelines, Vision-Language-Action (VLA) models [5]–[13] unify perception, task un-

This work is supported by the National Natural Science Foundation of China under Grant 62173189. This work is done during internship of Yifan Yang, Tianshi Xie, Fuyu Cao, Pinxi Shen at Xiaomi EV.

¹The Institute of Robotics and Automatic Information System, Tianjin Key Laboratory of Intelligent Robotics, and TBI center, Nankai University, Tianjin 300350, China. Emails: yangyifan@mail.nankai.edu.cn; li-ujt@nankai.edu.cn.

²Xiaomi EV, Beijing, China.

³Faculty of Robot Science and Engineering, Northeastern University, Shenyang 110819, China

⁴The State Key Laboratory of Internet of Things for Smart City, and Centre for Artificial Intelligence and Robotics, and Department of Electromechanical Engineering, University of Macau, Macau SAR, China.

*Corresponding author. † Project leader.

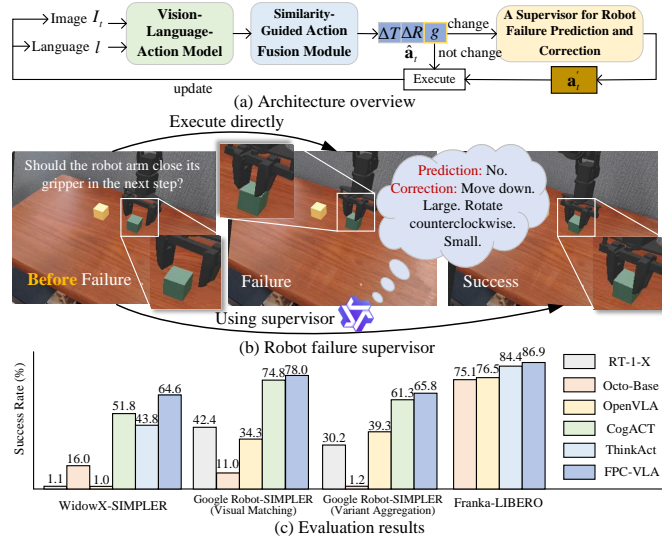


Fig. 1. We propose FPC-VLA, a dual-model framework that integrates VLA with a supervisor for failure prediction and correction. It outperforms other advanced methods in all benchmarks.

derstanding, and motion generation into a single model, directly mapping visual observations and natural language instructions into low-level robot actions. By leveraging large-scale pretraining on vision-language data, such models can generalize across diverse objects, environments, and ambiguous commands without relying on explicit 3D modeling, which enables zero-shot or few-shot adaptation to new tasks. Additionally, the model dynamically infers tasks from language, enhancing intuitive human-robot interaction.

Despite the significant progress in VLA models, current frameworks still face several notable limitations. First, as shown in Fig. 1(a), most existing approaches [5]–[13] rely heavily on imitation learning from expert demonstrations, which are typically composed only of successful trajectories. This leads to a fundamental weakness: these models struggle to recover from deviations, often requiring external supervision for potential failure prediction and corrective guidance. Moreover, collecting large-scale datasets that capture both failure prediction and correction is another bottleneck. Most existing datasets usually annotate failures post hoc [14]–[17], and rarely enable early prediction or proactive interventions. The lack of a standardized or scalable methodology limits the model’s generalization ability. In addition, as shown in Fig. 1(b), many current methods segment actions into action chunks, losing the information of the latter part of

the predicted sequence, and often overlook the multimodal nature of action trajectories—i.e., the fact that there may be multiple plausible ways to achieve a goal.

To address these challenges, we propose FPC-VLA, a vision-language-action framework with a supervisor for failure prediction and correction. A VLM-based supervisor verifies predicted actions before execution and, if necessary, provides directional corrections to refine motion. We also introduce an automated method to generate a large-scale failure prediction and correction dataset from RLDS-format data, pairing images, task instructions, and gripper-focused QA prompts. Additionally, a similarity-guided action fusion module is proposed to aggregate historical predictions using cosine similarity and temporal decay, producing smoother and more robust action outputs.

The main contributions of this work are as follows:

- 1) We propose a VLM-based supervisor that predicts and corrects potential robot failures by evaluating gripper actions using structured prompts and image inputs.
- 2) We introduce a similarity-guided action fusion module that aggregates historical predictions to produce smoother and more reliable robotic motions.
- 3) We evaluate FPC-VLA on SIMPLER and LIBERO benchmarks, using WidowX, Google Robot and Franka, and test it for real-world applicability on real robots. The results show that FPC-VLA outperforms other state-of-the-art methods.

II. RELATED WORK

A. Vision-Language-Action Models

Recent advances in multi-modal learning have driven the development of VLAs. Notable early examples include RT-1 [5], RT-2 [6], and RT-X [7], which enable end-to-end training on large datasets, achieving strong generalization across platforms. Open-source models like Octo [8] and OpenVLA [9] have also emerged, pre-trained on extensive robot datasets and fine-tuned with domain-specific data. More recent efforts, such as SpatialVLA [10] with Ego3D encoding and adaptive action grids, and TraceVLA [11] with visual trace prompting, enhance spatial and spatiotemporal reasoning. Other developments include RoboVLMs [12], which use continuous outputs and policy heads, and CogACT [13], which employs diffusion action transformers for modeling action sequences. Despite these advances, VLA models still struggle with autonomously detecting and recovering from failures in unstructured environments.

B. Robot Failure Detection and Correction

To address robot failure challenges, recent studies have explored using Multimodal Large Language Models (MLLMs) as auxiliary agents for error detection and reasoning. [14] can identify the reasons for failure, but does not provide a correction strategy. [18] implements failure correction but relies on human-provided instructions. [15]–[17] are able to autonomously adjust strategies after grasping failures, but lack the ability to anticipate such failures beforehand. Among them, RACER [16] also uses an external supervisor, but it

only provides a corrected task instruction in natural language after a failure, which cannot be directly mapped to action changes. EvolvingGrasp [19] improves through preference alignment from both successes and failures, and Phoenix [20] connects semantic reflection with motion-level correction. Unlike the approaches primarily focusing on post-failure adaptations or manual intervention, our approach anticipates failure scenarios and provides preemptive corrective actions.

III. METHOD

A. Architecture Overview and Problem Formulation

As shown in Fig. 2, the input to FPC-VLA consists of an RGB image $I_t \in \mathbb{R}^{H \times W \times 3}$ and a language instruction l at timestep t . The output is a refined action $\hat{\mathbf{a}}_t \in \mathbb{R}^7$ that corrects failure-prone predictions. The proposed pipeline includes three modules: 1) a robot failure dataset generation method, 2) a VLM-based supervisor for failure prediction and correction, and 3) a similarity-guided action fusion module.

In the dataset generation module, grasp events are identified by detecting changes in gripper state g_t , forming a change set \mathcal{C} . For each event $c \in \mathcal{C}$, we retain frames \mathcal{R}_c , and compute pose differences $\Delta \mathbf{a}$. These are converted into structured language descriptions using thresholds $\delta_{\text{trans}}^{\text{small}}, \delta_{\text{trans}}^{\text{large}}, \delta_{\text{rot}}^{\text{small}}, \delta_{\text{rot}}^{\text{large}}$, and combined with task and answer constraints to form prompts \mathcal{P}_t . In the similarity-guided action fusion module, a set of past predictions \mathcal{A}_t is collected, each decomposed as $\mathbf{a}_t^{(k)} = [\mathbf{p}_t^{(k)}, g_t^{(k)}]$ in observation \mathcal{O}_{t-k} . Cosine similarity $\text{sim}^{(k)}$ with the latest pose $\mathbf{p}_t^{(0)}$ is smoothed via sigmoid $s^{(k)}$, weighted by time decay $d^{(k)}$, and normalized to produce fusion weights $w^{(k)}$, yielding the fused action $\hat{\mathbf{a}}_t = [\hat{\mathbf{p}}_t, \hat{g}_t]$. In the VLM-based failure prediction and correction module, when g_t changes, the model \mathcal{M} takes image I_t and prompt \mathcal{P}_t as input, returning response $R_t = \mathcal{M}(I_t, \mathcal{P}_t)$. If R_t starts with “No”, translation correction $\Delta \mathbf{p} \in \mathbb{R}^3$ and rotation correction $\Delta r_z \in \mathbb{R}$ are extracted to obtain refined action $\hat{\mathbf{a}}'_t$.

B. Vision-Language-Action Model

Vision Module The vision module is responsible for extracting patch-level features from input images and projecting them into the embedding space of the language model. Given image I_t , it is passed through hybrid visual encoder built on DINOv2 [21] and SigLIP [22]. The encoded features are then passed through a linear projection to align with the LLM embedding space to get vision tokens $\mathcal{V} = \{v_1, v_2, \dots, v_{N_V}\}$. **Language Module** The language module is built on Llama2 [23], a transformer-based architecture designed for autoregressive language modeling. The input consists of a sequence of language tokens $\mathcal{L} = \{l_1, l_2, \dots, l_{N_L}\}$, where each token l_i is mapped to a high-dimensional embedding space \mathbb{R}^d . For multimodal inputs, the text embeddings \mathcal{L} are combined with visual embeddings \mathcal{V} from the vision module. The output cognition token $\mathcal{Z} \in \mathbb{R}^d$ is used as input for the action module to interpret and generate the required actions. **Action Module** The action module uses Diffusion Transformer (DiT) [24] to generate action sequences conditioned

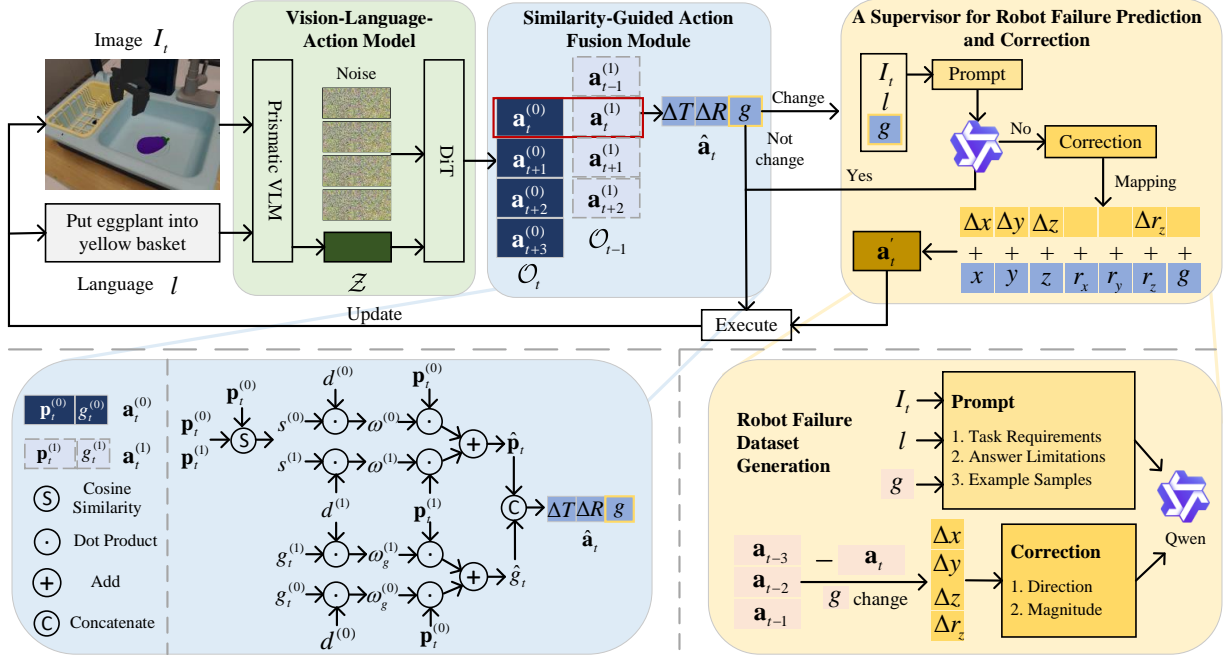


Fig. 2. Architecture of FPC-VLA. The input to the framework consists of the observed image and a natural language instruction, and the output is the end-effector pose increment and the gripper state of the robotic arm.

on \mathcal{Z} . Diffusion model generates actions by gradually denoising a noisy input, while the transformer backbone enhances the model’s ability to capture long-range dependencies in the data. During the training phase, the noisy sample x_t is obtained using the q-sampling process

$$x_t = \sqrt{\alpha_t} \cdot x_0 + \sqrt{1 - \alpha_t} \cdot \epsilon, \quad (1)$$

where $\alpha_t \in (0, 1)$ controls the noise level at timestep t , and x_0 represents the ground truth actions for the next n steps. The model DiT is trained to predict the noise ϵ added to x_0 , given the noisy input x_t , the timestep t , and the condition \mathcal{Z}

$$\text{DiT}(x_t, t, z) \approx \epsilon. \quad (2)$$

C. Robot Failure Prediction and Correction Dataset

Most existing large-scale VLA datasets [5], [7], [25], [26] only include successful trajectories, while current failure correction datasets [15], [17] are limited in scale and lack predictability. To address this, we propose an automated method for generating failure correction datasets from large-scale RLDS-format data and adapt them for VLM training.

Denote the dataset \mathcal{D} as a collection of episodes. Each episode \mathcal{E}_i consists of a sequence of steps

$$\mathcal{D} = \{\mathcal{E}_1, \mathcal{E}_2, \dots, \mathcal{E}_N\}, \quad \mathcal{E}_i = \{s_1, s_2, \dots, s_T\}, \quad (3)$$

where each step s_t includes:

- An RGB image observation $I_t \in \mathbb{R}^{H \times W \times 3}$,
- An action vector $\mathbf{a}_t \in \mathbb{R}^7$ (6-DOF pose + 1-D gripper),
- A task-level language instruction l .

Discrete grasp events are detected by tracking changes in the gripper state g_t . The set of change timesteps is

$$\mathcal{C} = \{t \mid |g_t - g_{t-1}| > \delta_g\}, \quad (4)$$

where the threshold δ_g is 0.5. For each change timestep $c \in \mathcal{C}$, retain a set of three preceding frames and itself

$$\mathcal{R}_c = \{c-3, c-2, c-1, c\} \cap [1, T]. \quad (5)$$

The total set of retained indices is $\mathcal{R} = \bigcup_{c \in \mathcal{C}} \mathcal{R}_c$.

For every retained frame s_t with $t \in \mathcal{R}$, we identify the next change timestep $c \in \mathcal{C}$ such that $c \geq t$, and compute the pose difference

$$\Delta \mathbf{a} = \mathbf{a}_c - \mathbf{a}_t. \quad (6)$$

For each $\Delta \mathbf{a}$, we construct a textual description based on movement and rotation direction. For each axis $i \in \{x, y, z\}$, a movement direction and magnitude are defined as

$$T_i = \begin{cases} \text{None,} & |\Delta i| \leq \delta_{\text{trans}}^{\text{small}} \\ \text{Move } D. \text{ Small,} & \delta_{\text{trans}}^{\text{small}} < |\Delta i| \leq \delta_{\text{trans}}^{\text{large}} \\ \text{Move } D. \text{ Large,} & |\Delta i| > \delta_{\text{trans}}^{\text{large}} \end{cases}. \quad (7)$$

Around the vertical axis z , a rotation direction is defined similarly as

$$R = \begin{cases} \text{None,} & |\Delta r_z| \leq \delta_{\text{rot}}^{\text{small}} \\ \text{Rotate } D. \text{ Small,} & \delta_{\text{rot}}^{\text{small}} < |\Delta r_z| \leq \delta_{\text{rot}}^{\text{large}} \\ \text{Rotate } D. \text{ Large,} & |\Delta r_z| > \delta_{\text{rot}}^{\text{large}} \end{cases}, \quad (8)$$

where $\delta_{\text{trans}}^{\text{small}}, \delta_{\text{trans}}^{\text{large}}, \delta_{\text{rot}}^{\text{small}}, \delta_{\text{rot}}^{\text{large}}$ are thresholds that limit the magnitude of movement or rotation, $\Delta i = i_{t+1} - i_t$ represents the position change along the i -th axis, and D is the direction. Table I illustrates the correspondence between variables and directions using the BridgeV2 [25] dataset as an example.

Given the retained frame s_t , a standard prompt \mathcal{P}_t consists of three parts: task requirements, answer limitations, and example samples. An example is shown in Table II.

TABLE I

MAPPING OF VARIABLES AND DIRECTIONS IN BRIDGEV2 DATASET

Axis	Variable	Sign	Direction D
X	Δx	+	forward
		-	backward
Y	Δy	+	left
		-	right
Z	Δz	+	up
		-	down
Around Z	Δr_z	+	counterclockwise
		-	clockwise

TABLE II

EXAMPLE OF FAILURE PREDICTION AND CORRECTION PROMPTS

Part	Content
Task Requirements	My task is to pick rxbar chocolate from bottom drawer and place on counter. Should the robot arm close its gripper in the next step? If not, please specify the direction and magnitude of the gripper’s movement and rotation.
Answer Limitations	The direction must be chosen from the following options: move up, move down, move left, move right, rotate clockwise, and rotate counterclockwise. At most one option can be selected from each pair: move up or move down, move left or move right, and rotate clockwise or rotate counterclockwise. The magnitude should be either large or small. Your response should start with ‘Yes’ or ‘No’. If the answer is ‘No’, then include the direction and magnitude of both movement and rotation.
Example Samples	Here are some example responses: Example 1: Yes. Example 2: No. Move up. Large. Move left. Small. Example 3: No. Move down. Large. Rotate clockwise. Small.

D. A VLM-Based Supervisor for Robot Failure Prediction and Correction

Existing robotic manipulation systems based on VLA models often directly execute predicted commands without assessing their contextual appropriateness. These systems typically lack the ability to predict the consequences of actions or to autonomously correct erroneous decisions. To address this limitation, we propose a failure prediction and correction supervisor that evaluates the suitability of gripper actions before execution.

Let the predicted action at timestep t be denoted as:

$$\hat{\mathbf{a}}_t = [x_t, y_t, z_t, r_{x,t}, r_{y,t}, r_{z,t}, g_t], \quad (9)$$

where $(x, y, z) \in \mathbb{R}^3$ is the desired end-effector position delta. $(r_x, r_y, r_z) \in \mathbb{R}^3$ is the rotation delta. g is the gripper command (0 for close, 1 for open). Here, $\hat{\mathbf{a}}_t$ comes from the output of the action fusion module in Section III-E.

The framework checks gripper consistency by comparing the current g_t and previous g_{t-1} . The robot failure prediction and correction supervisor is triggered when the difference exceeds the threshold δ_g

$$|g_t - g_{t-1}| > \delta_g. \quad (10)$$

When the gripper state g_t meets the condition in (10), the prompt \mathcal{P}_t and the current image I_t are input into a vision language model \mathcal{M}

$$R_t = \mathcal{M}(I_t, \mathcal{P}_t), \quad (11)$$

where R_t represents the generated natural language response by the model \mathcal{M} .

If the response R_t is “Yes.”, it indicates that \mathcal{M} approves the decision made by VLA regarding the opening or closing of the gripper, and the action will continue. If R_t begins with “No”, the action $\hat{\mathbf{a}}_t$ needs to be adjusted according to the modification suggestions provided by \mathcal{M} . In the latter case, we extract structured directives from the text, including translation correction $\Delta \mathbf{p} \in \mathbb{R}^3$ and rotation correction $\Delta r_z \in \mathbb{R}$, based on predefined directional mappings. Each directional token is paired with a discrete magnitude indicator (small or large), which is mapped to a scalar step size ($\delta_{\text{trans}}^{\text{small}}$ or $\delta_{\text{trans}}^{\text{large}}$, $\delta_{\text{rot}}^{\text{small}}$ or $\delta_{\text{rot}}^{\text{large}}$). Based on the language-guided correction, we generate a refined action

$$\mathbf{a}'_t = \hat{\mathbf{a}}_t + [\Delta x, \Delta y, \Delta z, 0, 0, \Delta r_z, 0], \quad (12)$$

leaving unaffected components unchanged. The refined action \mathbf{a}'_t is then executed within the environment.

E. Similarity-Guided Action Fusion Module

To obtain a robust and smooth action output and avoid waste in action prediction, we employ an action fusion strategy. At each timestep t , the output action $\hat{\mathbf{a}}_t$ is not solely determined by the most recent policy output, but rather by fusing a set of historical predictions, each made from earlier observations. This strategy fully takes into account the multimodality and temporal properties of actions, as well as the differences in pose and gripper states.

Let \mathcal{O}_{t-k} denote the observation at time $t-k$, and let $\mathbf{a}_t | \mathcal{O}_{t-k}$ represent the model’s prediction for the action at time t , based solely on the observation available at time $t-k$. We denote this prediction as

$$\mathbf{a}_t^{(k)} := \mathbf{a}_t | \mathcal{O}_{t-k}. \quad (13)$$

We collect a set of such predictions from the past N time steps

$$\mathcal{A}_t = \left\{ \mathbf{a}_t^{(k)} \mid k = 0, 1, \dots, N-1 \right\}. \quad (14)$$

Each $\mathbf{a}_t^{(k)} \in \mathbb{R}^7$ is decomposed as $\mathbf{a}_t^{(k)} = [\mathbf{p}_t^{(k)}, g_t^{(k)}]$, where $\mathbf{p}_t^{(k)} \in \mathbb{R}^6$ represents the relative end-effector pose, and $g_t^{(k)} \in \mathbb{R}$ denotes the scalar gripper state.

Using the most recent prediction $\mathbf{p}_t^{(0)}$ as a reference, we calculate the cosine similarity between each $\mathbf{p}_t^{(k)}$ and $\mathbf{p}_t^{(0)}$

$$\text{sim}^{(k)} = \frac{\mathbf{p}_t^{(k)} \cdot \mathbf{p}_t^{(0)}}{\|\mathbf{p}_t^{(k)}\| \cdot \|\mathbf{p}_t^{(0)}\| + \varepsilon}, \quad (15)$$

where $\varepsilon = 10^{-7}$ is a small constant for numerical stability. To smooth the similarity response and ensure differentiability, we apply a sigmoid transformation with a scaling factor $\alpha > 0$

$$s^{(k)} = \sigma(\alpha \cdot \text{sim}^{(k)}). \quad (16)$$

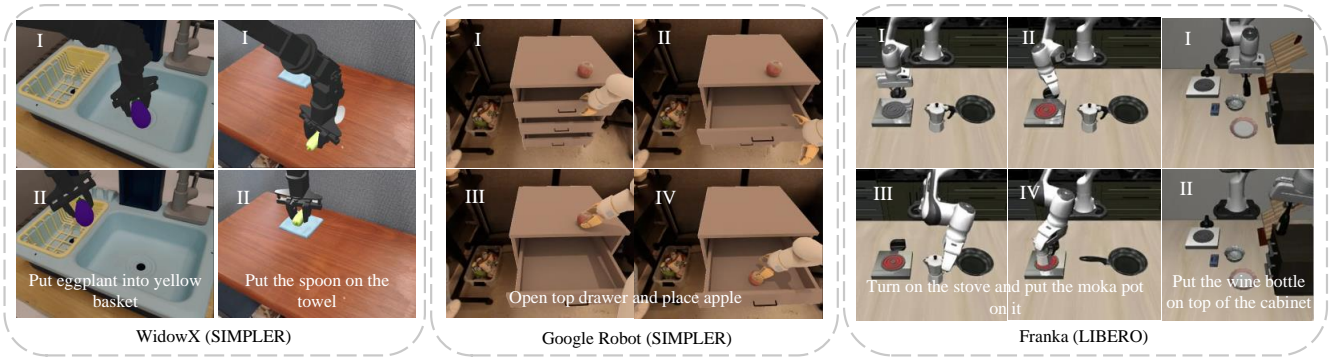


Fig. 3. Simulation results of FPC-VLA on different robots. The model performs well even in long-horizon tasks and non-pick-and-place tasks (e.g., opening drawers and turning on the stove).

This yields similarity weights $s^{(k)} \in (0, 1)$ that reflect the semantic alignment between the current and past predictions. We intentionally exclude g_t from the cosine similarity computation due to semantic misalignment, magnitude disparity, and behavioral decoupling — as the gripper often functions independently of the end-effector pose (e.g., holding an object steady while the arm moves).

To give higher importance to recent predictions, we apply an exponential decay over time

$$d^{(k)} = \exp(-\lambda \cdot k), \quad (17)$$

where $\lambda > 0$ is a decay coefficient. The total weight $w^{(k)}$ for each pose is then computed as the product of similarity and temporal decay

$$w^{(k)} = \frac{\max(0, (1 - \beta) \cdot s^{(k)} \cdot d^{(k)})}{\sum_{j=0}^{N-1} \max(0, (1 - \beta) \cdot s^{(j)} \cdot d^{(j)})}, \quad (18)$$

where $\beta \in [0, 1)$ is a regularization factor that prevents overconfidence in a small subset of predictions.

The final fused pose is computed as the weighted average

$$\hat{\mathbf{p}}_t = \sum_{k=0}^{N-1} w^{(k)} \cdot \mathbf{p}_t^{(k)}. \quad (19)$$

For the scalar gripper state g_t , we intentionally do not apply similarity-based weighting, because the cosine similarity measure is computed based on \mathbf{p}_t , and does not meaningfully reflect the behavior or intent of g_t . Instead, we use temporal decay alone to perform a weighted average over historical gripper values

$$\hat{g}_t = \sum_{k=0}^{N-1} \tilde{d}^{(k)} \cdot g_t^{(k)}, \quad \text{where } \tilde{d}^{(k)} = \frac{d^{(k)}}{\sum_{j=0}^{N-1} d^{(j)}}. \quad (20)$$

The final output action $\hat{\mathbf{a}}_t$ is a concatenation of the fused pose and gripper state $\hat{\mathbf{a}}_t = [\hat{\mathbf{p}}_t, \hat{g}_t] \in \mathbb{R}^7$.

IV. EXPERIMENT

A. Implementation Details

The VLM model of FPC-VLA adopts Prismatic VLMs [30]. The VLM model of the supervisor uses Qwen2.5-vl 7B [31]. During training, we use 8 NVIDIA H100 GPUs. For

the VLA model, the batch size is set to 256, the learning rate is 2×10^{-5} , and 15 action steps are predicted per inference. For the supervisor model, training is conducted with bfloat16 precision, a batch size of 64, a learning rate of 10^{-4} , LoRA rank of 8, LoRA alpha of 32, and max pixels of 1003520. During inference, for WidowX, the supervisor is trained on dataset generated from BridgeV2 [25] (408771 entries), with $\delta_{\text{trans}}^{\text{small}}, \delta_{\text{trans}}^{\text{large}}, \delta_{\text{rot}}^{\text{small}}, \delta_{\text{rot}}^{\text{large}}$ set to 0.001, 0.01, 0.001, and 0.01 respectively, and the size of action window $N = 7$. For Google Robot, dataset is generated from [5] (728760 entries), with $\delta_{\text{trans}}^{\text{small}}, \delta_{\text{trans}}^{\text{large}}, \delta_{\text{rot}}^{\text{small}}, \delta_{\text{rot}}^{\text{large}}$ set to 0.01, 0.1, 0.01, and 0.1 respectively, and $N = 2$. For Franka, dataset is generated from [26] (15604 entries), with $\delta_{\text{trans}}^{\text{small}}, \delta_{\text{trans}}^{\text{large}}, \delta_{\text{rot}}^{\text{small}}, \delta_{\text{rot}}^{\text{large}}$ set to 0.01, 0.1, 0.001, and 0.01 respectively. $N = 5$ for the goal setting, $N = 7$ for the spatial setting, and $N = 11$ for others. In action fusion module, $\alpha = 0.1$, $\lambda = \beta = 0.01$. Supervisor is called no more than 3 times in each task.

FPC-VLA achieves inference time of 0.176s for non-keyframes and 1.766s for keyframes. As the supervisor is called at most three times during the hundreds of inferences per task, its benefit becomes more evident in long-horizon tasks. For example, in the Open Top Drawer and Place Apple task, the total inference time of FPC-VLA is 40.5 s, which is only slightly higher than the 35.2 s when the supervisor is inactive.

B. Evaluation on Simulation Benchmarks

To evaluate the FPC-VLA model, we conduct experiments on two simulation platforms—SIMPLER [32] and LIBERO [26]—as well as on three types of robotic arms: WidowX, Google Robot, and Franka. On SIMPLER, we primarily highlight FPC-VLA’s zero-shot learning capability, using only pre-training on the OXE dataset [7] without domain-specific fine-tuning. On LIBERO, we focus on comparing the performance with other methods after fine-tuning. All evaluation tasks follow [11]–[13], [27].

Evaluation on SIMPLER SIMPLER [32] is an open-source suite of simulated environments to evaluate policies. Visual Matching reduces the visual disparity by overlaying real-world backgrounds and adjusting object textures to align with real environments. Variant Aggregation introduces

TABLE III
COMPARISON RESULTS ON SIMPLER WITH WIDOWX

Method	Fine-tuned (in-domain)	Put spoon on towel		Put carrot on plate		Stack green block on yellow block		Put eggplant on yellow basket		Avg. Grasp	Avg. Success
		Grasp	Success	Grasp	Success	Grasp	Success	Grasp	Success		
RT-1-X [7]	✗	16.7	0.0	20.8	4.2	8.3	0.0	0.0	0.0	11.5	1.1
Octo-Base [8]	✗	34.7	12.5	52.8	8.3	31.9	8.3	66.7	43.1	46.5	16.0
Octo-Small [8]	✗	77.8	47.2	27.8	9.7	40.3	4.2	87.5	56.9	58.4	29.5
OpenVLA [9]	✗	4.1	0.0	33.3	0.0	12.5	0.0	8.3	4.1	14.6	1.0
RoboVLMs [12]	✓	70.8	45.8	33.3	20.8	54.2	4.2	91.7	79.2	62.5	37.5
CogACT [13]	✗	–	71.7	–	50.8	–	15.0	–	67.5	–	51.8
SpatialVLA [10]	✗	25.0	20.8	41.7	20.8	58.3	25.0	79.2	70.8	51.2	34.4
SpatialVLA [10]	✓	20.8	16.7	29.2	25.0	62.5	29.2	100.0	100.0	53.1	42.7
ThinkAct [27]	✓	–	58.3	–	37.5	–	8.7	–	70.8	–	43.8
FPC-VLA	✗	79.2	79.2	58.3	58.3	70.8	45.8	79.2	75.0	71.9	64.6

TABLE IV
COMPARISON RESULTS ON SIMPLER WITH GOOGLE ROBOT

Method	Fine-tuned (in-domain)	Visual Matching				Open Top Drawer and Place Apple (108)	Average	Variant Aggregation				Average
		Pick Coke Can (300)	Move Near (240)	Open/Close Drawer (216)	Open/Close Drawer (378)			Pick Coke Can (825)	Move Near (600)	Open/Close Drawer (378)	Open Top Drawer and Place Apple (189)	
RT-1 [5]	✓	85.7	44.2	73.0	6.5	52.4	89.8	50.0	32.3	2.6	43.7	
RT-1-X [7]	✗	56.7	31.7	59.7	21.3	42.4	49.0	32.3	29.4	10.1	30.2	
RT-2-X [7]	✗	78.7	77.9	25.0	3.7	46.3	82.3	79.2	35.3	20.6	54.4	
Octo-Base [8]	✗	17.0	4.2	22.7	0.0	11.0	0.6	3.1	1.1	0.0	1.2	
OpenVLA [9]	✗	18.0	56.3	63.0	0.0	34.3	60.8	67.7	28.8	0.0	39.3	
RoboVLMs [12]	✓	77.3	61.7	43.5	24.1	41.9	–	–	–	–	–	
CogACT [13]	✗	91.3	80.5	71.8	50.9	74.8	89.6	80.8	28.3	46.6	61.3	
SpatialVLA [10]	✗	81.0	69.6	59.3	–	–	89.5	72.7	41.8	–	–	
SpatialVLA [10]	✓	86.0	77.9	57.4	–	–	88.0	72.7	41.8	–	–	
ThinkAct [27]	✓	92.0	72.4	50.0	–	–	84.0	63.8	47.6	–	–	
FPC-VLA	✗	95.3	93.8	76.4	46.3	78.0	91.3	86.7	30.7	54.5	65.8	

TABLE V
COMPARISON RESULTS ON LIBERO WITH FRANKA

Method	Goal	Spatial	Object	Long	Average
Diffusion [28]	68.3	78.3	82.5	50.5	72.4
Octo-Base [8]	84.6	78.9	85.7	51.1	75.1
OpenVLA [9]	79.2	84.7	88.4	53.7	76.5
TravceVLA [11]	75.1	84.6	85.2	54.1	74.8
SpatialVLA [10]	78.6	88.2	89.9	55.5	78.1
ThinkAct [27]	87.1	88.3	91.4	70.9	84.4
Cot-VLA [29]	87.6	87.5	91.6	69.0	81.1
FPC-VLA	86.2	87.0	92.0	82.2	86.9

multiple randomized variations in the simulation’s visual elements. In SIMPLER, we test FPC-VLA on two commonly used robotic platforms: WidowX and Google Robot. Visual results can be found in Fig. 3.

WidowX is tested for grasping, stacking blocks, and placing items into containers. Each task is repeated 24 times under varying object poses. Table III compares various methods with FPC-VLA, reporting performance in success rates (%). RT-1-X [7] and OpenVLA [9] perform poorly across most tasks, with task success rates near 0%, indicating difficulty in generalization due to domain gaps. Notably, FPC-VLA even outperforms the fine-tuned SpatialVLA [10] under the zero-shot setting, demonstrating its effectiveness in both grasping and task completion across varied manipulation scenarios.

Google Robot evaluation includes pick-and-place operations and drawer opening/closing tasks. Each task is repeated

under varying object poses and distractors. The number of attempts for each task is indicated in parentheses in Table IV. As shown in Table IV, in Visual Matching category, FPC-VLA achieves an average score of 78.0%, outperforming all baselines, despite in zero-shot setting. For Variant Aggregation tasks, which evaluates the ability to generalize across variants, FPC-VLA again ranks highest. It is worth noting that RT-1 [5] is trained solely on Google Fractal dataset [5], but FPC-VLA significantly outperforms it without any fine-tuning on that dataset. Even when faced with the most complex task (“Open Top Drawer and Place Apple” in Variant Aggregation setting), FPC-VLA still performs remarkably well, surpassing the results of other methods.

Evaluation on LIBERO LIBERO [26] simulation platform features four distinct task suites: LIBERO-Goal concentrates on achieving different task goals with fixed objects and spatial arrangements. LIBERO-Spatial focuses on adapting to varying spatial configurations of objects while maintaining object consistency. LIBERO-Object involves interacting with a diverse set of objects. LIBERO-Long contains long-horizon tasks that involve diverse objects, layouts, and goals.

Following the data modification and augmentation procedures from [9], we regenerate higher-resolution images (256x256px), remove no-op actions, rotate third-person images by 180°, filter out failed demonstrations, and use only third-person camera views for fair comparison. Each task suite is evaluated over 500 trials. As shown in Table

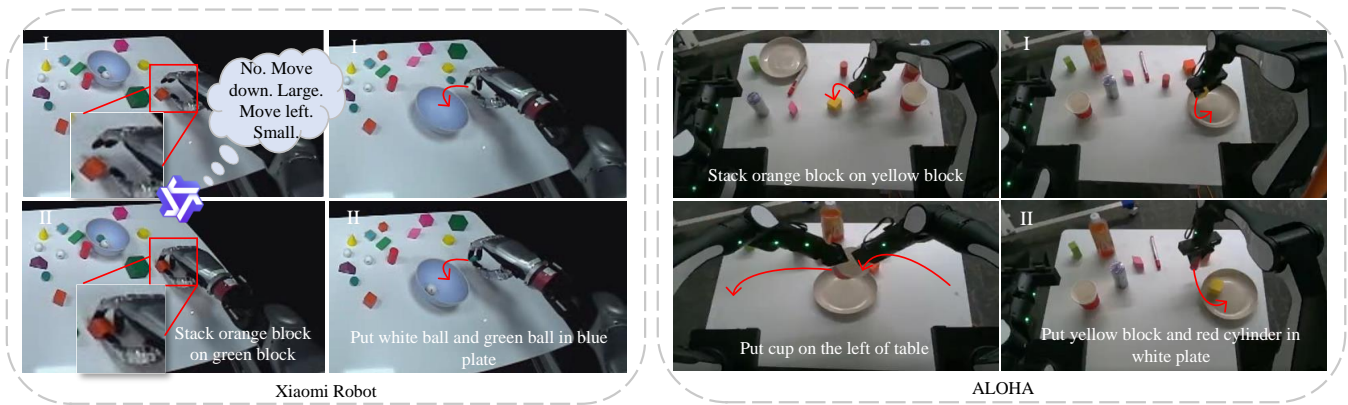


Fig. 4. Real world experiments results of FPC-VLA on Xiaomi Robot and ALOHA. Supervisor’s failure correction process is demonstrated taking the task “Stack orange block on green block” as an example.

TABLE VI
RESULTS OF ABLATION STUDY

Module	Setting	Put spoon on towel		Put carrot on plate		Stack green block on yellow block		Put eggplant on yellow basket		Avg. Grasp	Avg. Success
		Grasp	Success	Grasp	Success	Grasp	Success	Grasp	Success		
Supervisor	w/o Supervisor	83.3	75.0	62.5	50.0	50.0	37.5	79.2	70.8	50.0	58.3
	w/o correction	75.0	75.0	58.3	45.8	58.3	45.8	83.3	66.7	68.7	58.3
	w/o example samples	75.0	70.8	45.8	41.7	62.5	50.0	83.3	83.3	66.7	61.5
Action Fusion Module	use latest prediction	29.2	12.5	41.7	8.3	41.7	20.8	16.7	0	32.3	10.4
	directly average	79.2	79.2	58.3	54.2	62.5	50.0	83.3	66.7	70.8	62.5
	w/o time decay	79.2	70.8	50.0	37.5	58.3	33.3	79.2	66.7	66.7	52.1
motion disturbance + w/o Supervisor		62.5	54.2	50.0	41.7	50.0	20.8	37.5	25.0	50.0	35.4
motion disturbance + FPC-VLA		75.0	62.5	62.5	54.2	62.5	37.5	62.5	50.0	65.6	51.1
FPC-VLA		79.2	79.2	58.3	58.3	70.8	45.8	79.2	75.0	71.9	64.6

V, FPC-VLA achieves the highest average performance of 86.9%, significantly outperforming all other baselines. Notably, on the most challenging long-horizon tasks, it scores 82.2%, well above the second-best 70.9% by ThinkAct [27], indicating that failure prediction and correction can help avoid deviation in long-term tasks.

C. Real-World Experiments

To assess FPC-VLA’s real-world applicability, as shown in Fig. 4, we evaluate five challenging tasks on the Xiaomi Robot and ALOHA. Xiaomi Robot is a wheeled dual-arm system with 7-DoFs per arm, considering only the gripper’s open/close DoF. ALOHA has dual 6-DoF arms with parallel grippers. For each task, FPC-VLA is fine-tuned with 1000 in-domain demonstrations, while 1000 failure–correction pairs are used to fine-tune the supervisor. Inference uses FP16 on a single NVIDIA RTX 3090, with 32 trials per task. Results show that FPC-VLA achieves robust performance on long-horizon, cluttered tasks, with an average success rate of 86.3%. Notably, we include a dual-arm handover task (Put cup on the left of table), which demonstrates FPC-VLA’s versatility across multi-configuration robots.

D. Evaluation of Failure Prediction and Correction

To evaluate the accuracy of our supervisor’s failure prediction and correction, we compare it with several advanced

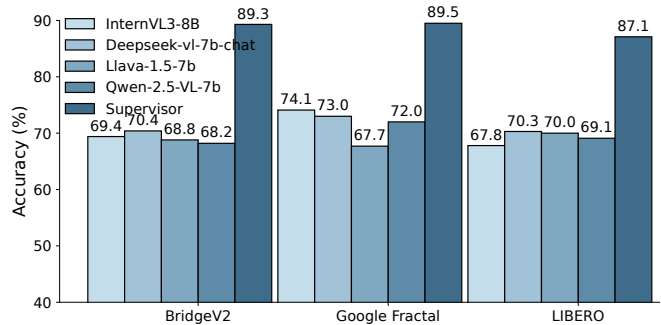


Fig. 5. Evaluation of failure prediction and correction accuracy between our supervisor and other advanced VLMs.

VLMs [31], [33]–[35]. Our supervisor is fine-tuned using the failure correction dataset generated as described in Section III-C, while the other VLMs use publicly available pretrained weights. As shown in Fig. 5, our supervisor outperforms all other methods on failure correction datasets derived from three different robotics datasets. Notably, our approach surpasses the base model Qwen2.5-VL-7B using only fine-tuning on generated data.

E. Ablation Study

Table VI presents the ablation study on FPC-VLA, focusing on the Supervisor and Action Fusion Module. “w/o” indi-

cates “without”. Results are measured on four WidowX tasks. Removing the Supervisor greatly degrades performance, as it corrects deviations from the expert trajectory. Removing corrections during data generation and inference also lowers success, indicating that VLM’s correction suggestions aid action optimization. Providing in-context examples further improves success by clarifying task requirements and output format. For the Action Fusion Module, similarity-guided fusion outperforms both no fusion and simple averaging by better leveraging multi-modal actions, while the time-decay strategy boosts success by emphasizing recent predictions.

To further evaluate the Supervisor’s effect on robustness, we perform an action perturbation experiment with and without the Supervisor. The end-effector pose is randomly disturbed within the range of [0.001, 0.01]. Results show that although perturbations reduce success rates in both settings, the drop is 39.3% without the Supervisor but only 20.9% with FPC-VLA.

V. CONCLUSION

In this paper, we propose FPC-VLA, a VLA Framework with a supervisor for failure prediction and correction. By integrating a VLM-based supervisor and a similarity-guided action fusion module, FPC-VLA not only refines robot actions before execution but also proactively mitigates potential failures. Extensive experiments across simulated environments and real-world robotic platforms demonstrate that FPC-VLA achieves superior performance over existing methods in both zero-shot and fine-tuned settings, highlighting its robustness, generalization ability, and potential for safe and reliable deployment in open-ended robotic applications.

REFERENCES

- [1] G. Wang, H. Li, S. Zhang, D. Guo, Y. Liu, and H. Liu, “Observe then act: Asynchronous active vision-action model for robotic manipulation,” *IEEE Robotics and Automation Letters*, vol. 10, no. 4, pp. 3422–3429, 2025.
- [2] Y. Zhang, T. Xue, A. Razmjoo, and S. Calinon, “Logic learning from demonstrations for multi-step manipulation tasks in dynamic environments,” *IEEE Robotics and Automation Letters*, vol. 9, no. 8, pp. 7214–7221, 2024.
- [3] Y. Yang, Z. Cui, Q. Zhang, and J. Liu, “Ps6d: Point cloud based symmetry-aware 6d object pose estimation in robot bin-picking,” in *2024 IEEE/RSJ International Conference on Intelligent Robots and Systems (IROS)*. IEEE, 2024, pp. 7167–7174.
- [4] Y. Yang, P. Song, E. Lan, D. Liu, and J. Liu, “Mk-pose: Category-level object pose estimation via multimodal-based keypoint learning,” *arXiv preprint arXiv:2507.06662*, 2025.
- [5] A. Brohan, N. Brown, J. Carbajal, Y. Chebotar, J. Dabis, C. Finn, K. Gopalakrishnan, K. Hausman, A. Herzog, J. Hsu *et al.*, “Rt-1: Robotics transformer for real-world control at scale,” *arXiv preprint arXiv:2212.06817*, 2022.
- [6] B. Zitkovich, T. Yu, S. Xu, P. Xu, T. Xiao, F. Xia, J. Wu, P. Wohlhart, S. Welker, A. Wahid *et al.*, “Rt-2: Vision-language-action models transfer web knowledge to robotic control,” in *Conference on Robot Learning*. PMLR, 2023, pp. 2165–2183.
- [7] A. O’Neill, A. Rehman, A. Maddukuri, A. Gupta, A. Padalkar, A. Lee, A. Pooley, A. Gupta, A. Mandlkar, A. Jain *et al.*, “Open x-embodiment: Robotic learning datasets and rt-x models: Open x-embodiment collaboration 0,” in *2024 IEEE International Conference on Robotics and Automation (ICRA)*. IEEE, 2024, pp. 6892–6903.
- [8] O. M. Team, D. Ghosh, H. Walke, K. Pertsch, K. Black, O. Mees, S. Dasari, J. Hejna, T. Kreiman, C. Xu *et al.*, “Octo: An open-source generalist robot policy,” *arXiv preprint arXiv:2405.12213*, 2024.
- [9] M. J. Kim, K. Pertsch, S. Karamcheti, T. Xiao, A. Balakrishna, S. Nair, R. Rafailov, E. Foster, G. Lam, P. Sanketi *et al.*, “Openvla: An open-source vision-language-action model,” *arXiv preprint arXiv:2406.09246*, 2024.
- [10] D. Qu, H. Song, Q. Chen, Y. Yao, X. Ye, Y. Ding, Z. Wang, J. Gu, B. Zhao, D. Wang *et al.*, “Spatialvla: Exploring spatial representations for visual-language-action model,” *arXiv preprint arXiv:2501.15830*, 2025.
- [11] R. Zheng, Y. Liang, S. Huang, J. Gao, H. Daumé III, A. Kolobov, F. Huang, and J. Yang, “Tracevla: Visual trace prompting enhances spatial-temporal awareness for generalist robotic policies,” *arXiv preprint arXiv:2412.10345*, 2024.
- [12] X. Li, P. Li, M. Liu, D. Wang, J. Liu, B. Kang, X. Ma, T. Kong, H. Zhang, and H. Liu, “Towards generalist robot policies: What matters in building vision-language-action models,” *arXiv preprint arXiv:2412.14058*, 2024.
- [13] Q. Li, Y. Liang, Z. Wang, L. Luo, X. Chen, M. Liao, F. Wei, Y. Deng, S. Xu, Y. Zhang *et al.*, “Cogact: A foundational vision-language-action model for synergizing cognition and action in robotic manipulation,” *arXiv preprint arXiv:2411.19650*, 2024.
- [14] J. Duan, W. Pumacay, N. Kumar, Y. R. Wang, S. Tian, W. Yuan, R. Krishna, D. Fox, A. Mandlkar, and Y. Guo, “Aha: A vision-language-model for detecting and reasoning over failures in robotic manipulation,” *arXiv preprint arXiv:2410.00371*, 2024.
- [15] Z. Luo, Y. Yang, C. Cai, Y. Zhang, and F. Zheng, “Roboreflex: Robotic reflective reasoning for grasping ambiguous-condition objects,” *arXiv preprint arXiv:2501.09307*, 2025.
- [16] Y. Dai, J. Lee, N. Fazeli, and J. Chai, “Racer: Rich language-guided failure recovery policies for imitation learning,” *arXiv preprint arXiv:2409.14674*, 2024.
- [17] W. Lu, M. Ye, Z. Ye, R. Tao, S. Yang, and B. Zhao, “Robofac: A comprehensive framework for robotic failure analysis and correction,” *arXiv preprint arXiv:2505.12224*, 2025.
- [18] L. Xiaoyang Shi, Z. Hu, T. Z. Zhao, A. Sharma, K. Pertsch, J. Luo, S. Levine, and C. Finn, “Yell at your robot: Improving on-the-fly from language corrections,” *arXiv e-prints*, pp. arXiv–2403, 2024.
- [19] Y. Zhu, Y. Zhong, Z. Yang, P. Cong, J. Yu, X. Zhu, and Y. Ma, “Evolvinggrasp: Evolutionary grasp generation via efficient preference alignment,” *arXiv preprint arXiv:2503.14329*, 2025.
- [20] W. Xia, R. Feng, D. Wang, and D. Hu, “Phoenix: A motion-based self-reflection framework for fine-grained robotic action correction,” in *Proceedings of the Computer Vision and Pattern Recognition Conference*, 2025, pp. 6981–6990.
- [21] M. Oquab, T. Darcet, T. Moutakanni, H. Vo, M. Szafraniec, V. Khalidov, P. Fernandez, D. Haziza, F. Massa, A. El-Nouby *et al.*, “Dinov2: Learning robust visual features without supervision,” *arXiv preprint arXiv:2304.07193*, 2023.
- [22] X. Zhai, B. Mustafa, A. Kolesnikov, and L. Beyer, “Sigmoid loss for language image pre-training,” in *Proceedings of the IEEE/CVF international conference on computer vision*, 2023, pp. 11 975–11 986.
- [23] H. Touvron, L. Martin, K. Stone, P. Albert, A. Almahairi, Y. Babaei, N. Bashlykov, S. Batra, P. Bhargava, S. Bhosale *et al.*, “Llama 2: Open foundation and fine-tuned chat models,” *arXiv preprint arXiv:2307.09288*, 2023.
- [24] W. Peebles and S. Xie, “Scalable diffusion models with transformers,” in *Proceedings of the IEEE/CVF international conference on computer vision*, 2023, pp. 4195–4205.
- [25] H. R. Walke, K. Black, T. Z. Zhao, Q. Vuong, C. Zheng, P. Hansen-Estruch, A. W. He, V. Myers, M. J. Kim, M. Du *et al.*, “Bridgedata v2: A dataset for robot learning at scale,” in *Conference on Robot Learning*. PMLR, 2023, pp. 1723–1736.
- [26] B. Liu, Y. Zhu, C. Gao, Y. Feng, Q. Liu, Y. Zhu, and P. Stone, “Liberor: Benchmarking knowledge transfer for lifelong robot learning,” *Advances in Neural Information Processing Systems*, vol. 36, pp. 44 776–44 791, 2023.
- [27] C.-P. Huang, Y.-H. Wu, M.-H. Chen, Y.-C. F. Wang, and F.-E. Yang, “Thinkact: Vision-language-action reasoning via reinforced visual latent planning,” *arXiv preprint arXiv:2507.16815*, 2025.
- [28] C. Chi, Z. Xu, S. Feng, E. Cousineau, Y. Du, B. Burchfiel, R. Tedrake, and S. Song, “Diffusion policy: Visuomotor policy learning via action diffusion,” *The International Journal of Robotics Research*, p. 02783649241273668, 2023.
- [29] Q. Zhao, Y. Lu, M. J. Kim, Z. Fu, Z. Zhang, Y. Wu, Z. Li, Q. Ma, S. Han, C. Finn *et al.*, “Cot-vla: Visual chain-of-thought reasoning

- for vision-language-action models,” in *Proceedings of the Computer Vision and Pattern Recognition Conference*, 2025, pp. 1702–1713.
- [30] S. Karamcheti, S. Nair, A. Balakrishna, P. Liang, T. Kollar, and D. Sadigh, “Prismatic vlms: Investigating the design space of visually-conditioned language models,” in *Forty-first International Conference on Machine Learning*, 2024.
- [31] S. Bai, K. Chen, X. Liu, J. Wang, W. Ge, S. Song, K. Dang, P. Wang, S. Wang, J. Tang *et al.*, “Qwen2. 5-vl technical report,” *arXiv preprint arXiv:2502.13923*, 2025.
- [32] X. Li, K. Hsu, J. Gu, K. Pertsch, O. Mees, H. R. Walke, C. Fu, I. Lunawat, I. Sieh, S. Kirmani, S. Levine, J. Wu, C. Finn, H. Su, Q. Vuong, and T. Xiao, “Evaluating real-world robot manipulation policies in simulation,” in *Proceedings of the Conference on Robot Learning (CoRL)*, 2024.
- [33] Q. Zhu, D. Guo, Z. Shao, D. Yang, P. Wang, R. Xu, Y. Wu, Y. Li, H. Gao, S. Ma *et al.*, “Deepseek-coder-v2: Breaking the barrier of closed-source models in code intelligence,” *arXiv preprint arXiv:2406.11931*, 2024.
- [34] J. Zhu, W. Wang, Z. Chen, Z. Liu, S. Ye, L. Gu, H. Tian, Y. Duan, W. Su, J. Shao *et al.*, “Internvl3: Exploring advanced training and test-time recipes for open-source multimodal models,” *arXiv preprint arXiv:2504.10479*, 2025.
- [35] H. Liu, C. Li, Y. Li, and Y. J. Lee, “Improved baselines with visual instruction tuning,” in *Proceedings of the IEEE/CVF conference on computer vision and pattern recognition*, 2024, pp. 26 296–26 306.